Genome-wide schizophrenia variant at *MIR137* does not impact white matter microstructure in healthy participants

Sinead Kelly[a,b], Derek W. Morris[a,f], Omar Mothersill[a,b], Emma Jane Rose[a,b,c], Ciara Fahey[a,b], Carol O'Brien[a,b], Erik O'Hanlon[d], Michael Gill[a,b], Aiden P. Corvin[a,b], Gary Donohoe[a,b,e,*]

[a] Neuropsychiatric Genetics Group, Department of Psychiatry, Trinity Centre for health Sciences, St. James's Hospital, Dublin 8, Ireland
[b] Trinity College Institute for Neuroscience, Trinity College Dublin, Ireland
[c] Transdisciplinary Science and Translational Prevention Program (TSTPP), Research Triangle Institute, Baltimore, MD, United States
[d] Department of Psychiatry, Royal College of Surgeons in Ireland, Ireland
[e] School of Psychology, National University of Ireland Galway, Ireland
[f] Discipline of Biochemistry, School of Natural Sciences, National University of Ireland Galway, Ireland

ABSTRACT

A single nucleotide polymorphism (SNP rs1625579) within the micro-RNA 137 (*MIR137*) gene recently achieved strong genome-wide association with schizophrenia (SZ). However, the mechanisms by which SZ risk may be mediated by this variant are unknown. As miRNAs have the potential to influence oligodendrocyte development, we investigated whether this SNP was associated with variability in white matter (WM) microstructure. Diffusion tensor imaging (DTI) was conducted on 123 healthy participants genotyped for rs1625579. The analysis consisted of whole-brain tract-based spatial statistics and atlas-based tractography analysis of six major WM tracts known to be affected in SZ – the inferior longitudinal fasciculus, the uncinate fasciculus, the inferior fronto-occipital fasciculus, the anterior thalamic radiation, the cingulum bundle and the corpus callosum. No significant differences in either whole-brain fractional anisotropy or mean diffusivity between *MIR137* genotype groups were observed ($p > 0.05$). Similarly, atlas-based tractography of particular tracts implicated in SZ failed to reveal any significant differences between *MIR137* genotype groups on measures of WM connectivity ($p > 0.05$). In the absence of WM effects comparable to those reported for other SZ associated genes, these data suggest that *MIR137* alone may not confer variability in these WM measures and therefore may not act in isolation for any effects that the variant may have on WM microstructure in SZ samples

1. Introduction

Compromised white matter (WM) integrity is a widely replicated finding in schizophrenia (SZ) pathophysiology [1] with a meta-analysis revealing two aberrant WM networks, firstly in the frontal lobe consisting of WM interconnecting the frontal lobe, thalamus and cingulate gyrus and, secondly, a network in the temporal WM interconnecting the frontal lobule, insula, hippocampus-amygdala and occipital lobe [2]. An abundance of evidence suggests that these WM abnormalities SZ are heritable, for example WM abnormalities are apparent in first-degree relatives, individuals at high risk of SZ, and in patients during the early stages of illness [3–5]. Therefore, WM connectivity is potentially an appropriate endophenotype (i.e. a variation occurring on the pathway between

* Corresponding author at: School of Psychology, National University of Ireland, Galway, Ireland. Tel.: +353 91493002.
E-mail address: gary.donohoe@NUIGalway.ie (G. Donohoe).

genes and disease phenotype) for delineating the mechanisms of genetic risk in SZ [6].

A single nucleotide polymorphism (SNP) rs1625579, within an intron of the micro-RNA 137 (*MIR137*) host gene showed the strongest genome-wide association for SZ in one of the largest genome-wide association studies (GWAS) to date [7]. *MIR137* regulates maturation and migration of adult neural stem cells [8] and is expressed in the subventricular layers and subgranular layer of the hippocampus [9]. It plays a critical role in neurogenesis and dendritic morphogenesis [9] and has also been shown to regulate other genes with genome-wide significance for SZ, including CACNA1C and TCF4 [10] that may be relevant for WM integrity and oligodendrocyte development [11–13]. In addition, miRNAs can act to prevent the expression of genes that promote oligodendrocyte precursor cell maintenance to inhibit proliferation and thus promote differentiation [14]. Therefore, evidence suggests that *MIR137* may regulate genes that have the potential to affect WM development.

A recent investigation conducted by Lett and colleagues [15] found in a neuroimaging sample of 92 SZ patients and 121 healthy controls, that the risk T allele homozygote patients displayed decreases in whole-brain fractional anisotropy (FA) throughout the WM skeleton using tract-based spatial statistics (TBSS). This effect was observed in the patient sample only. Considering miRNAs have the ability to promote oligodendrocyte development, and as *MIR137* regulates other SZ genes that may be crucial for the development of WM, confirming whether *MIR137*'s effect on WM are general or specific to SZ patients remains an important question. The purpose of the present study was to address this question in a comparable sample of healthy participants stratified by *MIR137* genotype. To expand on the previous study [15], we conducted region of interest (ROI) tractography on WM tracts known to be impacted by SZ (i.e. the inferior longitudinal fasciculus (ILF), uncinate fasciculus (UF), inferior frontal occipital fasciculus (IFOF), anterior thalamic radiation (ATR) the cingulum bundle (CB) and the corpus callosum (CC)), as well as whole-brain TBSS. We also evaluated potential effects of this variant on alternative measures of WM microstructure more sensitive to axonal density and myelination [16–18] including axial, radial and mean diffusivity, as well as FA. It was hypothesised that the risk 'T' allele at rs1625579 would be associated with compromised WM connectivity in those tracts that form frontal and temporal WM networks altered in SZ [2].

2. Methods

2.1. Participants

The DTI sample consisted of 152 healthy participants recruited from the general population through local advertising on volunteer websites and notice boards in a range of public places across Dublin city including colleges, restaurants, shops, libraries, art galleries, cinemas and hospitals. Twelve subjects were removed from analysis due to poor quality data (see Section 2.4). Of the sample remaining, 123 were successfully genotyped for *MIR137*. This sample had a mean age of 32.30 years (SD = 11.68). Participant demographics are presented in Table 1. All participants were genetically Irish (i.e. had Irish born paternal and maternal grandparents), were between 18 and 65 years of age and were right-handed. Written, informed consent was obtained from all subjects in accordance with local ethics committee guidelines. Exclusion criteria included a significant neurological or psychiatric history (i.e. loss of consciousness; head injury; history of seizures or epilepsy; diagnosis of a psychiatric illness; currently taking psychiatric medication; hospitalisation due to a psychiatric or neurological condition), a first-degree relative with a diagnosis of SZ or other psychosis, substance abuse in the preceding six months (screened for separately to psychiatric history), pregnancy or other contraindication for MRI. Participants were not paid for participation but were offered reimbursement for study related expenses.

2.2. Genotyping

The *MIR137* rs1625579 variant was genotyped using a Taqman® SNP genotyping assay on a 7900HT sequence detection system (Applied Biosystems) (see Supplementary material)

2.3. DTI

Magnetic resonance images were collected using a 3-T Philips Achieva scanner. DTI images were acquired via a single-shot spin-echo echo planar imaging (EPI) with diffusion sensitizing gradients applied sequentially along 15 non-collinear directions with a b-value of 800 s/mm^2 (TR = 12445 ms TE = 52 ms, FOV = 224 mm × 224 mm × 149 mm, acquisition matrix = 112 × 112, reconstruction matrix = 128 × 128, 60 slices, 2.2 mm slice thickness, slice gap = 0.299 mm, spatial resolution = 2 mm × 2 mm × 2.2 mm, flip angle = 90°).

2.4. Preprocessing

Using ExploreDTI software [19], diffusion data were converted to ExploreDTI*.mat files with a voxel size of 2 mm × 2 mm × 2 mm. Diffusion tensor estimation was weighted linear and was based on the least-squares (LS) regression model [20]. A cubic interpolation and robust estimation of tensors by outlier rejection (RESTORE) [21] was used to correct for subject motion and cardiac pulsation artifacts. Data processing also included eddy current correction and B-matrix rotation during realignment [22]. A visual inspection of the corrected diffusion data was then performed and residual and outlier profiles were also examined. Allowable movement during scanning was less than 2 mm in any direction and less than 3° rotation in axial, sagittal or coronal planes for all participants. A further nine subjects were excluded from the current sample due to excessive motion in the scanner.

2.5. Atlas-based tractography

Atlas-based deterministic tractography was conducted using ExploreDTI (v4.8.3). All data were transformed into Montreal Neurological Institute (MNI) space. A whole-brain WM tract construction was then carried out for each participant using a linear interpolation. Seed point resolution was set at 2 mm × 2 mm × 2 mm with a seed fractional anisotropy threshold of 0.2 and an angle threshold of 45 degrees. Particular tracts implicated in SZ (i.e. UF, ILF, IFOF, ATR, CB and CC) were isolated using the automated atlas based tractography segmentation tool known to yield robust and reliable tract delineation [23] (see Fig. 1).

The diffusivity indices including mean FA, AD, MD and RD for each participant were exported to PASW statistical software (Release 18; SPSS Inc., Chicago, IL, USA) and subjected to a one-way multivariate analysis of covariance with genotype group (GT/GG and TT) as fixed factors. The frequency of the minor 'G' allele is such that in our sample only two individuals were identified as 'G' homozygotes. Therefore, GT and GG carriers were collapsed into one group as previously conducted [24]. Age and gender did not significantly differ between genotype groups and therefore these variables were included as covariates of no interest in the analysis as a matter of standard protocol [25]. As FA, MD, RD and AD are constructed from the three eigenvalues of the tensor, a Bonferroni corrected alpha level of $p = 0.017$ was applied for testing of multiple diffusion measures arising from three eigenvalues.

Table 1
Participant demographics based on rs1625579 genotype (G is minor allele; T is associated allele).

MIR137 – rs1625579	*N*	N males	N females	Age (years; mean(SD))	Education (years; mean (SD))
GT/GG	41	17	24	31.63 (11.93)	16.9 (3.56)
TT	82	41	41	32.02 (11.62)	17.01 (3.17)
Total	123	58	65	32.30 (11.68)	16.97 (3.29)

2.6. Whole-brain TBSS

Voxel-wise tract-based spatial statistics (TBSS [26]) of the FA and MD data was performed using FSL v4.1.6 to determine if any potential genotype effects are specific to the tracts selected or if they are more generalised. All subjects' FA data were aligned to a common space using the nonlinear registration tool FNIRT [27,28] that uses a b-spline representation of the registration warp field [29]. Next, the mean FA image was created and thinned to produce a mean FA skeleton representing the centres of all tracts common to the group. Each subject's aligned FA data was projected onto this skeleton and the resulting data was fed into voxelwise cross-subject statistics. For MD data, FA images were used to achieve the nonlinear registration and skeletonisation stages, and also to estimate the projection from each individual subject onto the mean FA skeleton. The nonlinear warps and skeleton projection were then applied to MD data.

Statistical analysis for TBSS was conducted using FSL's 'Randomise' algorithm. Threshold-free cluster enhancement (TFCE) [30] was selected using 5000 permutations per test. For the two genotype groups, two one-way general linear model (GLM) *t*-test designs were set-up. The statistical threshold was set at $p < 0.05$, family-wise error (FWE) corrected for multiple comparisons across the whole brain to find differences between genotype groups.

3. Results

3.1. DTI

After FWE correction, no significant differences in whole-brain FA or MD between *MIR137* genotype groups remained significant ($p > 0.05$). Similarly, atlas-based tractography of particular tracts implicated in SZ revealed no significant differences between *MIR137* genotype groups on measures of FA, MD, AD or RD ($p > 0.05$).

4. Discussion

The rs1625579 SNP at *MIR137* remains one of the strongest genome-wide associated variants for SZ [7]. The association of this polymorphism with variation in cognition, brain structure, function, age-of-onset of psychosis, and SZ symptomology suggests that this gene affects established endophenotypes for SZ. Since variation of WM connectivity is considered a reliable SZ endophenotype, and miRNAs are implicated in oligodendrocyte development, we investigated if this variant may also confer risk for SZ via an impact of WM microstructure. WM microstructural variations associated with *MIR137* have been reported for SZ patients but not in healthy controls [15]. The present study aimed to expand on previous work by investigating whole-brain FA *and* MD, and conducting regionally specific tractography in tracts that are relevant to the SZ disease phenotype. It was our aim to determine whether a more extensive battery of tests of WM integrity may be sensitive to the effects of SZ risk variants, like *MIR137*/rs1625579, in the absence of confounding disease-specific effects, i.e. in healthy individuals. Our analyses were not indicative of an association between *MIR137* genotype and measures of FA, or MD, at a whole-brain level or for FA, MD, AD and RD at an ROI tract-based level. This expands on the previous findings [15] and lends support to the conclusion that *MIR137* may not impact WM independently of SZ diagnosis. Additional factors associated with illness including the presence of other risk variants, medication, as well as severity and duration of illness may contribute to previous *MIR137* patient effects [15].

Given the negative findings reported here, one important question to consider is whether our study was adequately powered to detect true differences associated with this variant. Post-hoc power analyses are not recommended [31], and therefore the power of our study to detect a particular effect size was calculated using G* Power 3 software [32] avoiding the use of *p* values and effect sizes generated from our own analysis. Corresponding to a one-tailed *t*-test with $p < 0.05$, it was calculated that the sample size of this study had 100% power to detect an effect of Cohen's $d = 0.7$ or greater and 90% power to detect a medium effect size of 0.55. This is in line with effect sizes found in previous imaging genetics studies utilizing DTI [6]. However, this sample size had only 50% power to detect an effect size of 0.3. On this basis, while the present analysis was underpowered to detect smaller effects, it would appear to have been adequately powered to detect effects of the size previously reported for other risk variants [6].

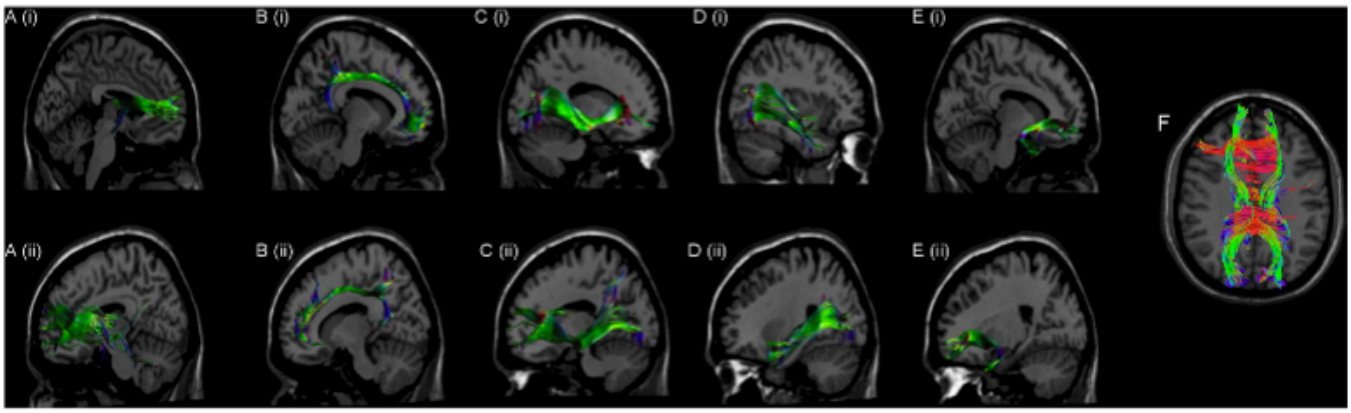

Fig. 1. Atlas-based deterministic tract reconstruction of the anterior thalamic radiation (ATR) (A, ii and i), cingulum bundle (CB) (B, i and ii), inferior fronto-occipital fasciculus (IFOF) (C, i and ii), inferior longitudinal fasciculus (ILF) (D, i and ii), uncinate fasciculus (UF) (E, i and ii) and the corpus callosum (CC) (F) for left and right hemispheres.

Another factor that may have contributed to our outcomes and should be considered is that our DTI data included just 15 gradient directions. Repeating this analysis using high-angular resolution data may be useful for characterizing complex crossing fibres in brain WM bundles. Measures such as FA, AD and RD are found to be sensitive to the presence of crossing fibres [33]. Crossing fibres are particularly problematic for tractography based on the diffusion tensor [34] as they can potentially cause the tracking algorithm to venture off course into an adjacent WM tract and this can result in both false-positive and false-negatives connections [35]. In addition, Sprooten and colleagues [36] also point out that DTI is not sensitive to more small-scale differences in structural integrity given the scale at which FA is measured, especially close to the synapse or near the grey matter, further away from large fibre bundles. There is also the potential issue of inter-subject variability or non-overlapping differences in this sample, particularly in the context of such a heterogeneous condition as SZ, which may have been overlooked by the DTI methods utilised. Although TBSS has attempted to address this issue, significant amounts of WM remain excluded particularly in areas that are not so rich in defined tracts [37]. Further analyses are required using more advanced techniques such as high-angular diffusion imaging (HARDI) and tractography conducted in native space to allow for more detailed exploration of regions that fall outside skeletonised WM in TBSS.

Finally, the latest SZ GWAS has identified another SNP at the same locus in a larger sample [38]. The SNP considered in this current analysis was selected prior to publication of this latest GWAS, however, both SNPs are in high linkage disequilibrium ($r^2 = 0.76$) and therefore it is unlikely that a potential association between these variants and WM microstructure in healthy participants has been discounted.

5. Conclusions

No significant effects of rs1625579 at *MIR137* were found in healthy individuals for either whole-brain TBSS and ROI tractography. This was true for measures of MD, RD and AD, as well as the more commonly used FA. This expands on the previous findings [15] and suggests that *MIR137* may not impact WM independently of SZ diagnosis. A recent study by our group found an association with this variant and altered functional connectivity during face processing in healthy controls [24]. Understanding potentially differential effects of *MIR137* on structural and functional connectivity will require a more detailed exploration of the variant's functional biology. Finally, a multi-variant or pathway approach is warranted to establish if this variant at *MIR137* is conferring risk for SZ via regulation of other SZ associated genetic variants.

Acknowledgments

We would like to thank all those individuals who participated in the study, and staff and students in the Trinity College Institute of Neuroscience involved in the collection of data. Finally, we would like to acknowledge data management support from the Trinity Centre for High Performance Computing. The data management system used for this work was BC|SNPmax v. 3.5-121 (Biocomputing Platforms Ltd, Finland). This work was generously supported by Science Foundation Ireland (SFI grant 12/IP/1359 to GD and SFI08/IN.1/B1916-Corvin to AC), and the Health Research Board (HRA/2009/197 to GD).

Appendix A. Supplementary data

Supplementary data associated with this article can be found, in the online version, at http://dx.doi.org/10.1016/j.neulet.2014.05.002.

References

[1] M. Kubicki, R. McCarley, C.F. Westin, H.J. Park, S. Maier, R. Kikinis, F.A. Jolesz, M.E. Shenton, A review of diffusion tensor imaging studies in schizophrenia, J. Psychiatry Res. 41 (2007) 15–30.
[2] I. Ellison-Wright, E. Bullmore, Meta-analysis of diffusion tensor imaging studies in schizophrenia, Schizophr. Res. 108 (2009) 3–10.
[3] H. Witthaus, M. Brune, C. Kaufmann, G. Bonner, S. Ozgurdal, Y. Gudlowski, A. Heinz, R. Klingebiel, G. Juckel, White matter abnormalities in subjects at ultra high-risk for schizophrenia and first-episode schizophrenic patients, Schizphr. Res. 102 (2008) 141–149.
[4] R. Pérez-Iglesias, D. Tordesillas-Gutierrez, G.J. Barker, P.K. McGuire, R. Roiz-Santianez, I. Mata, E.M. de Lucas, F. Quintana, J.L. Vazquez-Barquero, B. Crespo-Facorro, White matter defects in first episode psychosis patients: a voxelwise analysis of diffusion tensor imaging, Neuroimage 49 (2010) 199–204.
[5] P. Kochunov, D.C. Glahn, J.L. Lancaster, A.M. Winkler, S. Smith, P.M. Thompson, L. Almasy, R. Duggirala, P.T. Fox, J. Blangero, Genetics of microstructure of cerebral white matter using diffusion tensor imaging, Neuroimage 53 (2010) 1109–1116.
[6] O. Mothersill, S. Kelly, E.J. Rose, G. Donohoe, The effects of psychosis risk variants on brain connectivity: a review, Front. Psychiatry 3 (2012) 1–12.
[7] S. Ripke, A.R. Sanders, K.S. Kendler, D.F. Levinson, P. Sklar, P.A. Holmans, et al., Genome-wide association study identifies five new schizophrenia loci, Nat. Genet. 43 (2011) 969–976.
[8] K.E. Szulwach, X. Li, R.D. Smrt, Y. Li, Y. Luo, L. Lin, N.J. Santistevan, W. Li, X. Zhao, P. Jin, Cross talk between microRNA and epigenetic regulation in adult neurogenesis, J. Cell Biol. 189 (2010) 127–141.
[9] R.D. Smrt, K.E. Szulwach, R.L. Pfeiffer, X. Li, W. Guo, M. Pathania, Z.Q. Teng, Y. Luo, J. Peng, A. Bordey, P. Jin, X. Zhao, MicroRNA miR-137 regulates neuronal maturation by targeting ubiquitin ligase mind Bomb-1, Stem Cells 28 (2010) 1060–1070.
[10] E. Kwon, W. Wang, L.H. Tsai, Validation of schizophrenia-associated genes CSMD1, C10orf26, CACNA1C and TCF4 as miR-137 targets, Mol. Psychiatry 18 (2011) 11–12.
[11] C. Matute, Calcium dyshomeostasis in white matter pathology, Cell Calcium 47 (2010) 150–157.
[12] D.M. McTigue, R.B. Tripathi, The life, death, and replacement of oligodendrocytes in the adult CNS, J. Neurochem. 107 (2008) 1–19.
[13] B. Emery, Regulation of oligodendrocyte differentiation and myelination, Science 330 (2010) 779–782.
[14] X. He, Y. Yu, R. Awatramani, Q.R. Lu, Unwrapping myelination by microRNAs, Neuroscientist 18 (2012) 45–55.
[15] T.A. Lett, M.M. Chakavarty, D. Felsky, E.J. Brandl, A.K. Tiwari, V.F. Gonçalves, T.K. Rajji, Z.J. Daskalakis, H.Y. Meltzer, J.A. Lieberman, J.P. Lerch, B.H. Mulsant, J.L. Kennedy, A.N. Voineskos, The genome-wide supported microRNA-137 variant predicts phenotypic heterogeneity within schizophrenia, Mol. Psychiatry 18 (2013) 443–450.
[16] K.L. Narr, N. Hageman, R.P. Woods, L.S. Hamilton, K. Clark, O. Philips, D.W. Shattuck, R.F. Asarnow, A.W. Toga, K.H. Neuchterlein, Mean diffusivity: a biomarker for CSF-related disease and genetic liability effects in schizophrenia. Psychiatry Res. Neuroimaging 171(2009) 20–32.
[17] S.K. Song, J. Yoshino, T.Q. Le, S.J. Lin, S.W. Sun, A.H. Cross, R.C. Armstrong, Demyelination increases radial diffusivity in corpus callosum of mouse brain, Neuroimage 26 (2005) 132–140.
[18] S.K. Song, S.W. Sun, M.J. Ramsbottom, C. Chang, J. Russell, A.H. Cross, Dysmyelination revealed through MRI as increased radial (but unchanged axial) diffusion of water, Neuroimage 17 (2002) 1429–1436.
[19] A. Leemans, B. Jeurissen, J. Sijbers, D.K. Jones, ExploreDTI: a graphical toolbox for processing, analyzing, and visualizing diffusion MR data, Proc. Intl. Soc. Mag. Reson. Med. 17 (2009) 3537.
[20] P. Basser, J. Mattiello, D. LeBihan, Estimation of the effective self-diffusion tensor from the NMR spin echo, J. Magn. Reson. Imaging 103 (1994) 247–254.
[21] L.C. Chang, D.K. Jones, C. Pierpaoli, RESTORE. Robust estimation of tensors by outlier rejection, Magn. Reson. Med. 53 (2005) 1088–1095.
[22] A. Leemans, D.K. Jones, The B-matrix must be rotated when correcting for subject motion in DTI data, Magn. Reson. Med. 61 (2009) 1336–1349.
[23] J.S. Verhoeven, C.A. Sage, A. Leemans, W. Van Hecke, D. Callaert, R. Peeters, P. DeCock, L. Lagae, S. Sunaert, Construction of a stereotaxic DTI atlas with full diffusion tensor information for studying white matter maturation from childhood to adolescence using tractography-based segmentations, Hum. Brain Mapp. 31 (2010) 470–486.
[24] O. Mothersill, D.W. Morris, S. Kelly, E.K. Rose, C. Fahey, C. O'Brien, R. Lyne, R. Reilly, M. Gill, A.P. Corivn, G. Donohoe, Effects of MIR137 on fronto-amygdala functional connectivity, Neuroimage (2013), http://dx.doi.org/10.1016/j.neuroimage.2013.12.019
[25] G.A. Miller, J.P. Chapman, Misunderstanding analysis of covariance, J. Abnorm. Psychol. 110 (2001) 40–48.
[26] M. Smith, M. Jenkinson, H. Jonansen-Berg, D. Rueckert, T.E. Nichols, C.E. Mackay, K.E. Watkins, O. Ciccarelli, M.Z. Cader, P.M. Matthews, T.E. Behrens, Tract-based spatial statistics: voxelwise analysis of multi-subject diffusion data, Neuroimage 31 (2006) 1487–1505.
[27] J.L. Andersson, M. Jenkinson, S. Smith, J. Andersson, Non-linear optimisation, FMRIB Technical Report TR07JA1, 2007.

[28] J.L. Andersson, M. Jenkinson, S. Smith, Non-Linear Registration, aka Spatial Normalisation FMRIB Technical Report TR07JA2, FMRIB Analysis Group of the University of Oxford, 2007.
[29] D. Rueckert, L.I. Sonda, C. Hayes, D.L. Hill, M.O. Leach, D.J. Hawkes, Nonrigid registration using free-form deformations: application to breast MR images, IEEE Trans. Med. Imaging 18 (1999) 712–721.
[30] S. Smith, T. Nichols, Threshold-free cluster enhancement: Addressing problems of smoothing, threshold dependence and localisation in cluster inference, Neuroimage 44 (2009) 83–98.
[31] J.M. Hoenig, D.M. Heisey, The abuse of power: the pervasive fallacy of power calculations for data analysis, Am. Stat. 55 (2001) 1–5.
[32] F. Faul, E. Erdfelder, A.G. Lang, A. Buchner, G*Power 3: A flexible statistical power analysis program for the social, behavioral, and biomedical sciences – Springer, Behavior. Res. Methods 39 (2007) 175–191.
[33] C.A.M. Wheeler-Kingshott, M. Cercignani, About axial and radial diffusivities, Magn. Reson. Med. 61 (2009) 1255–1260.
[34] J.D. Tournier, S. Mori, A. Leemans, Diffusion tensor imaging and beyond, Magn. Reson. Med. 65 (2011) 1532–1556.
[35] T. Behrens, H.J. Berg, S. Jbabdi, M. Rushworth, M.W. Woolrich, Probabilistic diffusion tractography with multiple fibre orientations: what can we gain, Neuroimage 34 (2007) 144–155.
[36] E. Sprooten, A.M. MacIntosh, S.M. Lawrie, J. Hall, J.E. Sussmann, N. Dahmen, A. Konrad, M.E.M. Bastin, G. Winterer, An investigation of a genomewide supported psychosis variant in ZNF804A and white matter integrity in the human brain, Magn. Reson. Imaging 30 (2012) 1373–1380.
[37] A. Zalesky, Moderating registration misalignment in voxelwise comparisons of DTI data: a performance evaluation of skeleton projection, Magn. Reson. Imaging 29 (2011) 111–125.
[38] S. Ripke, C. O'Dushlaine, K. Chambert, J.L. Moran, A.K. Kahler, S. Akterin, S.E. Bergen, A.L. Collins, J.J. Crowley, M. Fromer, Y. Kim, S.H. Lee, P.K. Magnusson, N Sanchez, E.A. Stahl, S. Williams, N.R. Wray, K. Xia, F. Bettella, A.D. Borglum, B.K. Bulik-Sullivan, P. Cormican, N. Craddock, C. de Leeuw, N. Durmishi, M. Gill, V. Golimbet, M.L. Hamshere, P. Holmans, D.M. Hougaard, K.S. Kendler, K. Lin, D.W. Morris, O. Mors, P.B. Mortensen, B.M. Neale, F.A. O'Neill, M.J. Owen, M.P. Milovancevic, D. Posthuma, J. Powell, A.L. Richards, B.P. Riley, D. Ruderfer, D. Rujescu, E. Sigurdsson, T. Silagadze, A.B. Smit, H. Stefansson, S. Steinberg, J. Suvisaari, S. Tosato, M. Verhage, J.T. Walters; Multicenter Genetic Studies of Schizophrenia Consortium, D.F. Levinson, P.V. Gejman, K.S. Kendler, C. Laurent, B.J. Mowry, M.C. O'Donovan, M.J. Owen, A.E. Pulver, B.P. Riley, S.G. Schwab, D.B. Wildenauer, F. Dudbridge, P. Holmans, J. Shi, M. Albus, M. Alexander, D. Campion, D. Cohen, D. Dikeos, J. Duan, P. Eichhammer, S. Godard, M. Hansen, F.B. Lerer, K.Y. Liang, W. Maier, J. Mallet, D.A. Nertney, G. Nestadt, N. Norton, F.A. O'Neill, G.N. Papadimitriou, R. Ribble, A.R. Sanders, J.M. Silverman, D. Walsh, N.M. Williams, B. Wormley; Wormley; Psychosis Endophenotypes International Consortium, M.J. Arranz, S. Bakker, S. Bender, E. Bramon, D. Collier, B. Crespo-Facorro, J. Hall, C. Iyegbe, A. Jablensky, R.S. Kahn, L. Kalaydjieva, S. Lawrie, C.M. Lewis, K., Genome-wide association analysis identifies 13 new risk loci for schizophrenia. Nat. Genet. 45 (2014) 1150–1159.